

AD-A200 409

A TRIDENT SCHOLAR
PROJECT REPORT

NO. 155

DTIC FILE COPY

"Electron Irradiation-induced Defects in $\text{Al}_x\text{Ga}_{1-x}\text{As}$ "



DTIC
ELECTE
NOV 03 1988
S D
VH

UNITED STATES NAVAL ACADEMY
ANNAPOLIS, MARYLAND

This document has been approved for public
release and sale; its distribution is unlimited.

11 00 005

UNCLASSIFIED

SECURITY CLASSIFICATION OF THIS PAGE (When Data Entered)

REPORT DOCUMENTATION PAGE		READ INSTRUCTIONS BEFORE COMPLETING FORM
1. REPORT NUMBER U.S.N.A. - TSPR: no. 155	2. GOVT ACCESSION NO.	3. RECIPIENT'S CATALOG NUMBER
4. TITLE (and Subtitle) ELECTRON IRRADIATION-INDUCED DEFECTS IN $\text{Al}_{1-x}\text{Ga}_x\text{AS}$	5. TYPE OF REPORT & PERIOD COVERED Final 1977/88	
	6. PERFORMING ORG. REPORT NUMBER	
7. AUTHOR(s) Wesley I. Summers	8. CONTRACT OR GRANT NUMBER(s)	
9. PERFORMING ORGANIZATION NAME AND ADDRESS United States Naval Academy, Annapolis.	10. PROGRAM ELEMENT, PROJECT, TASK AREA & WORK UNIT NUMBERS	
11. CONTROLLING OFFICE NAME AND ADDRESS United States Naval Academy, Annapolis.	12. REPORT DATE 10 June 1988	
	13. NUMBER OF PAGES 26	
14. MONITORING AGENCY NAME & ADDRESS (if different from Controlling Office)	15. SECURITY CLASS. (of this report)	
	15a. DECLASSIFICATION/DOWNGRADING SCHEDULE	
16. DISTRIBUTION STATEMENT (of this Report) This document has been approved for public release; its distribution is UNLIMITED.		
17. DISTRIBUTION STATEMENT (of the abstract entered in Block 20, if different from Report)		
18. SUPPLEMENTARY NOTES Accepted by the U.S. Trident Scholar Committee.		
19. KEY WORDS (Continue on reverse side if necessary and identify by block number) Semiconductors Defects Point defects		
20. ABSTRACT (Continue on reverse side if necessary and identify by block number) This study analyzed two Liquid Phase Epitaxy (LPE) grown $\text{Al}_{1-x}\text{Ga}_x\text{AS}$ samples. One sample was electron irradiated with 1 MeV electrons, the other sample was non-irradiated. The goal of this study was to see the effect of the electron irradiation and characterize any trapping states encountered. Deep Level Transient Spectroscopy (DLTS) was used to analyze the samples. Only one was encountered in the non-irradiated sample, the so called DX center [1], (OVER)		

UNCLASSIFIED

SECURITY CLASSIFICATION OF THIS PAGE (When Data Entered)

while eight states were found in the irradiated sample, including the DX center. From a discussion of the experimental results, it is concluded that the electron irradiation had no noticeable effect on the DX center, that the irradiation was responsible for the additional trapping states encountered in the irradiated sample, and that point defect modeling is accurate in characterizing the five of the seven irradiation-induced states. A summary of the DLTS trap parameters is given.

Plumbridge, G. A. et al. J. Appl. Phys. 61(10), 5000 (1987)



Accession For	
NTIS SPA&I	<input checked="" type="checkbox"/>
ITIS TAB	<input type="checkbox"/>
Unannounced	<input type="checkbox"/>
Distribution	
By	
Date Rec'd	
Filing Date	
Dist	
A-1	

S N 0102-LF-014-6601

UNCLASSIFIED

SECURITY CLASSIFICATION OF THIS PAGE (When Data Entered)

U.S.N.A. - Trident Scholar project report; no. 155 (1988)

"Electron Irradiation-induced Defects in $\text{Al}_x\text{Ga}_{1-x}\text{As}$ "


A Trident Scholar Project Report

by

Midshipman First Class Wesley I. Summers, Class of 1988

U. S. Naval Academy

Annapolis, Maryland


Advisor: Professor Robert N. Shelby
Physics Department

Accepted for Trident Scholar Committee


Chairperson


Date

ABSTRACT

This study analyzed two Liquid Phase Epitaxy (LPE) grown $\text{Al}_x\text{Ga}_{1-x}\text{As}$ samples. One sample was electron irradiated with 1 MeV electrons, the other sample was non-irradiated. The goal of this study was to see the effect of the electron irradiation and characterize any trapping states encountered. Deep Level Transient Spectroscopy (DLTS) was used to analyze the samples. Only one trap was encountered in the non-irradiated sample, the so called DX center [1], while eight states were found in the irradiated sample, including the DX center. From a discussion of the experimental results, it is concluded that the electron irradiation had no noticeable effect on the DX center, that the irradiation was responsible for the additional trapping states encountered in the irradiated sample, and that point defect modeling is accurate in characterizing the five of the seven irradiation-induced states. A summary of the DLTS trap parameters is given.

ACKNOWLEDGEMENTS

I would like to thank the following people for their encouragement and assistance in helping me complete this project. Professor L. L. Tankersley for helping with the word processing, Professor M. S. Korman for his encouraging words when things looked grim, the U. S. N. A. Physics Department laboratory support group headed by Mr. Norm Stead for their support in keeping the experimental gear working, Dr. Richard Magno from the Naval Research Labs for providing the semiconductor samples used in this study, and my classmates, particularly those in my company, for encouraging me to work hard and get things done. A special thanks is reserved for my advisor, Professor Robert N. Shelby, who continually complicated matters by saying, "Wes, can you explain what this means?", and who taught me several valuable lessons about experimental physics.

TABLE OF CONTENTS

Abstract	1
Acknowledgements	2
Table of Contents	3
I. Introduction	4
II. Theory	4
A. Depletion Region Physics	4
B. Emission Theory	6
C. Capacitance Transient	8
D. DLTS System	10
E. DLTS System Rate	10
F. $\text{Al}_x\text{Ga}_{1-x}\text{As}$ Sample History	11
III. Results and Analysis	11
A. Capacitance vs. Voltage Data	11
B. DLTS Data	12
IV. Conclusion	22
References	26

I. INTRODUCTION

The fact that semiconductor device speed and performance are affected by band gap defect energy states is well established. Abundant research has been and continues to be devoted to the characterization of these defect states or "traps". The goal of this type of research is to understand the basic physics of these traps in an effort to enhance device performance and guide device fabrication. III-V compounds like GaAs and $\text{Al}_x\text{Ga}_{1-x}\text{As}$ have been the focus of much attention in this field because their high switching rates make them ideal for microwave device and high-speed circuit applications. Electron irradiation of semiconductor samples introduces intrinsic defects, such as vacancies and interstitials, into the lattice structure in controllable amounts, and these defects can then be studied [2]. In this study, two samples of $\text{Al}_x\text{Ga}_{1-x}\text{As}$ grown by Liquid Phase Epitaxy from the same crystal, one electron irradiated, the other non-irradiated, were analyzed. The purpose was to compare the two samples to see the effect of the irradiation, and to characterize any trapping states encountered. The main technique used to study these samples was Deep Level Transient Spectroscopy, DLTS, developed by D. V. Lang in 1974 [3].

The report is separated into four sections beginning with this introduction and moving on to a section on applicable semiconductor theory, the data results and analysis section, and ending with a section on the conclusions drawn from this research.

II. THEORY

A. Depletion Region Physics

Most of the information obtained about trapping states arises from analysis of the physics of the depletion region, or space-charge layer, at a p^+n junction or Schottky barrier of a semiconductor. If one assumes that the impurity concentration changes abruptly from donor to acceptor, and that the acceptor concentration, N_A is much greater than the donor concentration, N_D , then one has as an abrupt p^+n junction. See Figure 1a. For the n-type

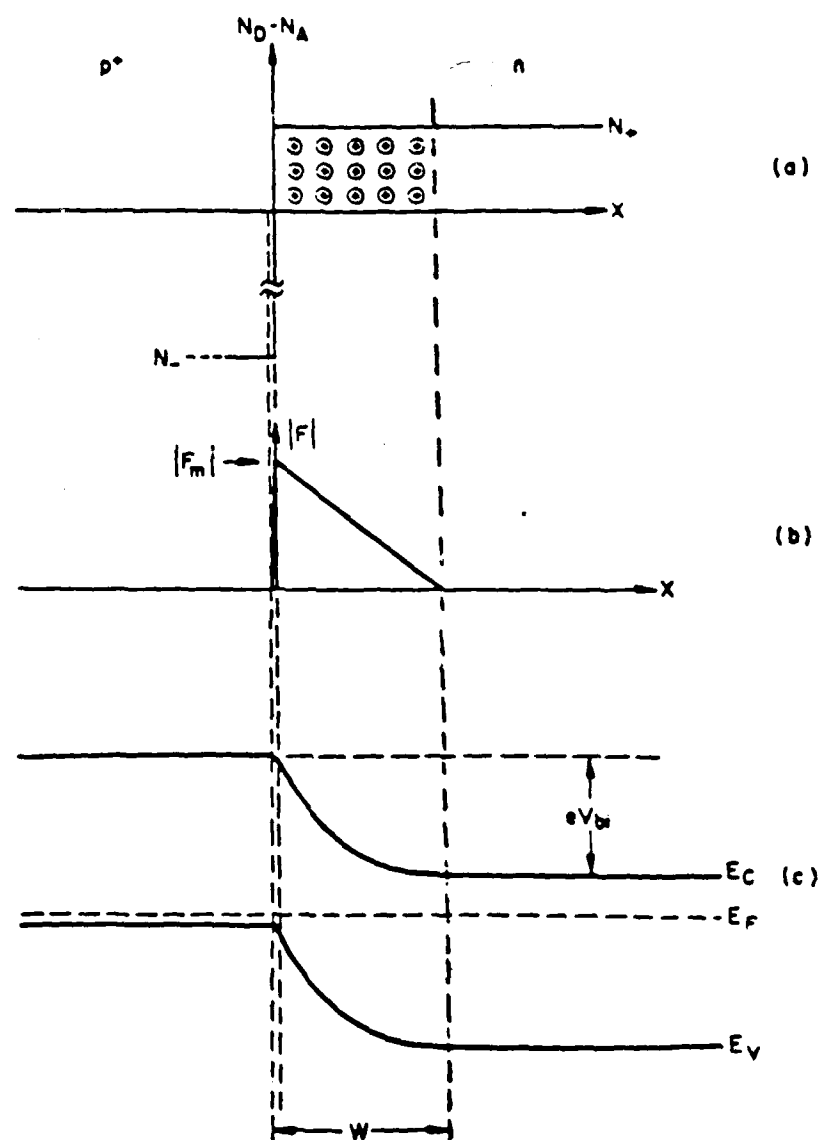


FIGURE 1: Ideal step junction (or n-type Schottky barrier) at zero bias (a) space charge distribution. (b) electric field distribution. (c) band-bending diagram.

Schottky barrier samples used, this is a valid assumption. Figure 1b and 1c show the electric field distribution and band bending diagram over the region. By solving Poisson's equation one obtains a relation for the depletion region width:

$$W = \sqrt{\frac{2\epsilon_s(V_{bi} + V_B)}{q(N_D + n_T)}} \quad (1)$$

where V_{bi} is the built-in voltage, V_B is the applied bias, ϵ_s is the permittivity, N_D is the ionized donor concentration, n_T is the ionized trap concentration, and q is the charge on the electron. If one defines $C = dQ_c/dV_B$ as the depletion region capacitance, where dQ_c is the change in charge per unit area for a given change in bias voltage dV_B , then rearranging equation (1) yields:

$$C = \frac{dQ_c}{dV_B} = \sqrt{\frac{q\epsilon_s(N_D + n_T)}{2(V_{bi} + V_B)}} \quad \text{pF/cm}^2 \quad (2)$$

Note that:

$$\frac{1}{C^2} = \frac{2}{q\epsilon_s(N_D + n_T)} (V_{bi} + V_B) \quad (3)$$

And:

$$\frac{d(1/C^2)}{dV_B} = \frac{2}{q\epsilon_s(N_D + n_T)} \quad (4)$$

Thus $1/C^2$ is proportional to V_B and the slope of the $1/C^2$ versus V_B curve is $2/q\epsilon_s(N_D + n_T)$ [4]. By taking capacitance versus bias voltage measurements one can obtain the background doping concentration for the sample.

B. Emission Theory

Since DLTS relies on the emission of carriers by traps to characterize trapping states, it is important to understand the physics of carrier emission. Transitions between a trap

and conduction band in equilibrium obey the principle that the emission rate is equal to the capture rate for a given trapping state (see Figure 2). The application of this principle and the use of Fermi-Dirac statistics leads to an expression for the emission rate of a group of traps.

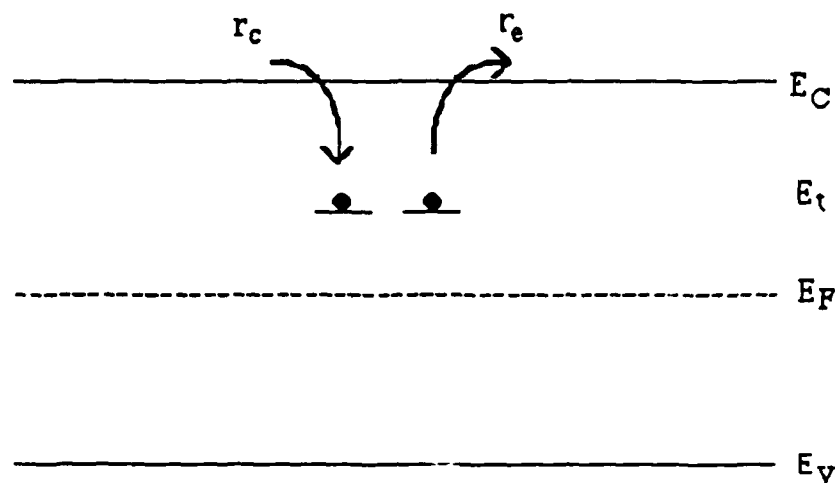


FIGURE 2: In thermodynamic equilibrium, the emission rate, r_e is equal to the capture rate, r_c .

The capture rate, r_c , and the emission rate r_e are given by:

$$r_c = \sigma v_{th} n_c [1 - f(E_t)] N_T \quad (5)$$

$$r_e = N_T R_t f(E_t) \quad (6)$$

where σ is the trap capture cross section, v_{th} is the thermal velocity, n_c is the number of electrons in the conduction band, $f(E_t)$ is the Fermi distribution, N_T is the trap concentration, and R_t is the trap emission rate. By setting these two expressions equal to each other, and substituting the Fermi distribution, one can solve for the trap emission rate:

$$R_t = v_{th} \sigma n_c e^{-\frac{E_t}{kT}} \quad (7)$$

where E_t is the energy difference between the conduction band and the sum of the trap energy and capture energy. The number of electrons in the conduction band and the thermal velocity are given by the following expressions, where k is the Boltzman constant and μ_e is the effective mass of the electron.

$$n_c = 2 \left[\frac{2\mu_e kT}{\hbar^2} \right]^{3/2} \quad v_{th} = \left[\frac{3kT}{\mu_e} \right]^{1/2} \quad (8, 9)$$

Substituting into equation 7 yields:

$$R_t = AT^2 e^{-(E_t/kT)} \quad (10)$$

where:

$$A = 4\sqrt{6} \frac{\mu_e k^2 \sigma}{\hbar^3} \quad (11)$$

Equation 10 gives the rate at which an electron will be emitted from a single trap with energy E_t at temperature T . By rearranging equation 10 and taking the natural log of both sides, one obtains the following expression:

$$\ln \left(\frac{T^2}{R_t} \right) = \left(\frac{E_t}{k} \right) \frac{1}{T} - \ln(A) \quad (12)$$

Note that this is a linear relation between the natural log of T^2/R and $1/T$. The slope is E_t/k and the intercept is the natural log of A . This type of plot is called an Arrhenius plot. Thus, if one can measure the emission rate of the trap, one can determine the trap energy and prefactor, A .

C. Capacitance Transient

Now that it has been shown that the rate of trap emission yields valuable information about trap parameters, it is important to understand how the capacitance transient measured by DLTS yields information on the trap concentration. As shown before in equation 2,

capacitance is proportional to the square root of the sum of the ionized donor and ionized trap concentrations. For the purpose of the following derivation, the constant of proportionality will be arbitrary, and denoted by γ . The capacitance at the end of the trap filling pulse is then given by the following expression:

$$C_0 = \gamma \sqrt{N_D} \quad (13)$$

And the capacitance at an infinite time after the filling pulse, i. e. a sufficient time for the traps to thermally emit their electrons is then:

$$C_\infty = \gamma \sqrt{N_D + N_T} \quad (14)$$

The capacitance at any time, t , after the filling pulse is:

$$C(t) = \gamma \sqrt{N_D + N_T(1 - e^{-R_t t})} \quad (15)$$

where N_T is the number of traps per cubic meter. Now let $\Delta C(t)$ be defined as the capacitance transient as a function of time, which is equal to $C(t) - C_\infty$. Substituting the above expressions and rearranging, one obtains the following relationship for the ratio of the transient capacitance to the quiescent capacitance.

$$\frac{\Delta C(t)}{C_\infty} = \sqrt{1 - \frac{N_T}{N_T + N_D} e^{-R_t t}} - 1 \quad (16)$$

Assume $N_T/(N_T + N_D) \ll 1$ and use the binomial expansion to obtain the following:

$$\frac{\Delta C(t)}{C_\infty} \approx -\frac{1}{2} \frac{N_T}{N_T + N_D} e^{-R_t t} \quad (17)$$

which evaluated at $t = 0$ and rearranged gives the approximate value for the trap concentration, N_T .

$$N_T \approx -\frac{2\Delta C_0}{C_\infty} N_D \quad \text{for } N_T \ll N_D \quad (18)$$

It has been shown [5] that a correction factor is needed to account for the traps that are

below the Fermi level in the depletion region, which don't participate in the capture or emission processes. The final expression for N_T is:

$$N_T = \frac{-2\Delta C_0}{C_\infty} N_D \left[\frac{V_{B1} + V_{bi}}{\left(\sqrt{V_{B1} + V_{bi}} - \sqrt{E_t}\right)^2 - \left(\sqrt{V_{B0} + V_{bi}} - \sqrt{E_t}\right)^2} \right] \quad (19)$$

where the applied bias pulse ranges from V_{B1} to V_{B0} .

D. DLTS System

The DLTS system used for this study is of the standard type [6]. There are, however, a few specifics that need to be mentioned before continuing on to the results section. The device used to sample the output transient signal is a waveform eductor, which averages the signal over one hundred channels whose parameters may be controlled by the operator. Temperature sweeps were made using a closed cycle helium refrigerator made by Air Products and Chemicals, Inc. which included a Model DE202 Expander Module and a Model K temperature controller with IEEE bus.

E. DLTS System Rate

A DLTS system generates a signal peak when the system emission rate corresponds to the trap emission rate. The following is the derivation of the emission rate of the system used in this study. Assuming an exponential transient capacitance signal,

$$S_1 = \Delta C_0 e^{-tR} \quad (20)$$

where ΔC_0 is the amplitude of the transient, and R is the emission rate. The signal generated by the I and J channels of the waveform eductor is then:

$$S_{I,J} = \frac{1}{TC} \int_{t_1}^{t_2} S_1 dt - \frac{1}{TC} \int_{t_3}^{t_4} S_1 dt \quad (21)$$

where: t_1 =start of channel I
 t_3 =start of channel J

t_2-t_1 =time of channel, TC
 t_4 =end of channel J

By integrating this equation and substituting in the appropriate parameters, the following expression is obtained for the waveform eductor signal as a fraction of ΔC_0 .

$$\frac{S_{I,J}}{\Delta C_0} = \frac{e^{-TD(R)}(e^{TC(R)} - 1)}{TC(R)} \left[e^{-I(TC)R} - e^{-J(TC)R} \right] \quad (22)$$

where TD is the time delay between the end of the bias pulse and the beginning of the first channel. A computer program, WFE.RATES, was used to find which R gave a maximum signal for a given I,J. This program also calculated the fraction of the signal to ΔC_0 which is needed to give the proper ΔC_0 for use in equation (19).

F. $Al_xGa_{1-x}As$ Sample History

The samples used in this study were grown by Liquid Phase Epitaxy. Both samples were grown from the same crystal. The aluminum fraction, x, for each sample is 0.3. The samples are of the Schottky barrier type. An n-type LPE $Al_xGa_{1-x}As$ layer was grown on an n-type GaAs substrate ($n=10^{18}$ 1/cm³) with a thin GaAs buffer layer ($n=10^{17}$ 1/cm³). The LPE layer was unintentionally doped at about $n=5 \times 10^{16}$ 1/cm³ with the most probable dopant being Si. The ohmic back was a Sn-Ag alloy and the Schottky pads were 15/1000 inch diameter gold. The samples were silicon capped and annealed at 800°C. One sample was then irradiated at 300K with 1MeV electrons to a fluence of 1×10^{16} electrons/cm². This sample was annealed a second time at 800°C. These samples will be referred to throughout the paper by their assigned laboratory codes. The non-irradiated sample code is S220-BB and the irradiated sample code is S220-BD.

Now that the background theory has been covered, it is time to look at the results of the data taking and analyze these results for relevant and reasonable conclusions.

III. RESULTS AND ANALYSIS

A. Capacitance vs. Voltage Data

Capacitance versus applied bias voltage measurements were made on each sample for a

variety of temperatures, ranging from 50K to 450K. These data sets were changed into $1/C^2$ vs. V_B curves from which slope was determined. A computer program was used to make a least-squares fit of each data point and the four points on each side of it. These computer generated slopes were then converted into a plot of the background doping, N_B , as a function of position, x , measured from the junction. Figure 3 shows a comparison of two such plots for S220BB and S220BD at 400K. Note that Figure 3 shows a decrease in the amount of background doping in the irradiated sample in comparison to the non-irradiated sample. This is caused by the capture of donor electrons by trapping states, electrons that would normally be emitted to the conduction band and swept out of the depletion region. Figure 4 shows several $N_B(x)$ plots for a range of temperatures for sample S220BD. Note that as more thermal energy is available at higher temperatures, more trapping states are ionized and a subsequent increase in N_B is observed. The following table is a compilation of the C-V data results, listing N_B for both samples and the ratio of $N_B(\text{S220BD})$ to $N_B(\text{S220BB})$ for several temperatures.

T(K)	N_B -S220BB	N_B -S220BD	N_B Ratio $\left\{ \frac{\text{S220BD}}{\text{S220BB}} \right\}$
50	$4.2 \times 10^{16} \text{ /cm}^3$	$2.2 \times 10^{16} \text{ /cm}^3$.52
100	5.5×10^{16}	3.0×10^{16}	.55
200	5.7×10^{16}	3.5×10^{16}	.61
300	6.8×10^{16}	3.8×10^{16}	.56
400	7.0×10^{16}	4.2×10^{16}	.60
450	7.5×10^{16}	5.0×10^{16}	.67

TABLE 1 : Summary of Capacitance vs. Bias Voltage Measurements

B. DLTS Data

After the capacitance-voltage measurements were completed, the next step was to begin the DLTS runs. The first runs on each sample were made by sweeping over the entire temperature range from about 20K to 450K. The goal of these first runs was see what kind

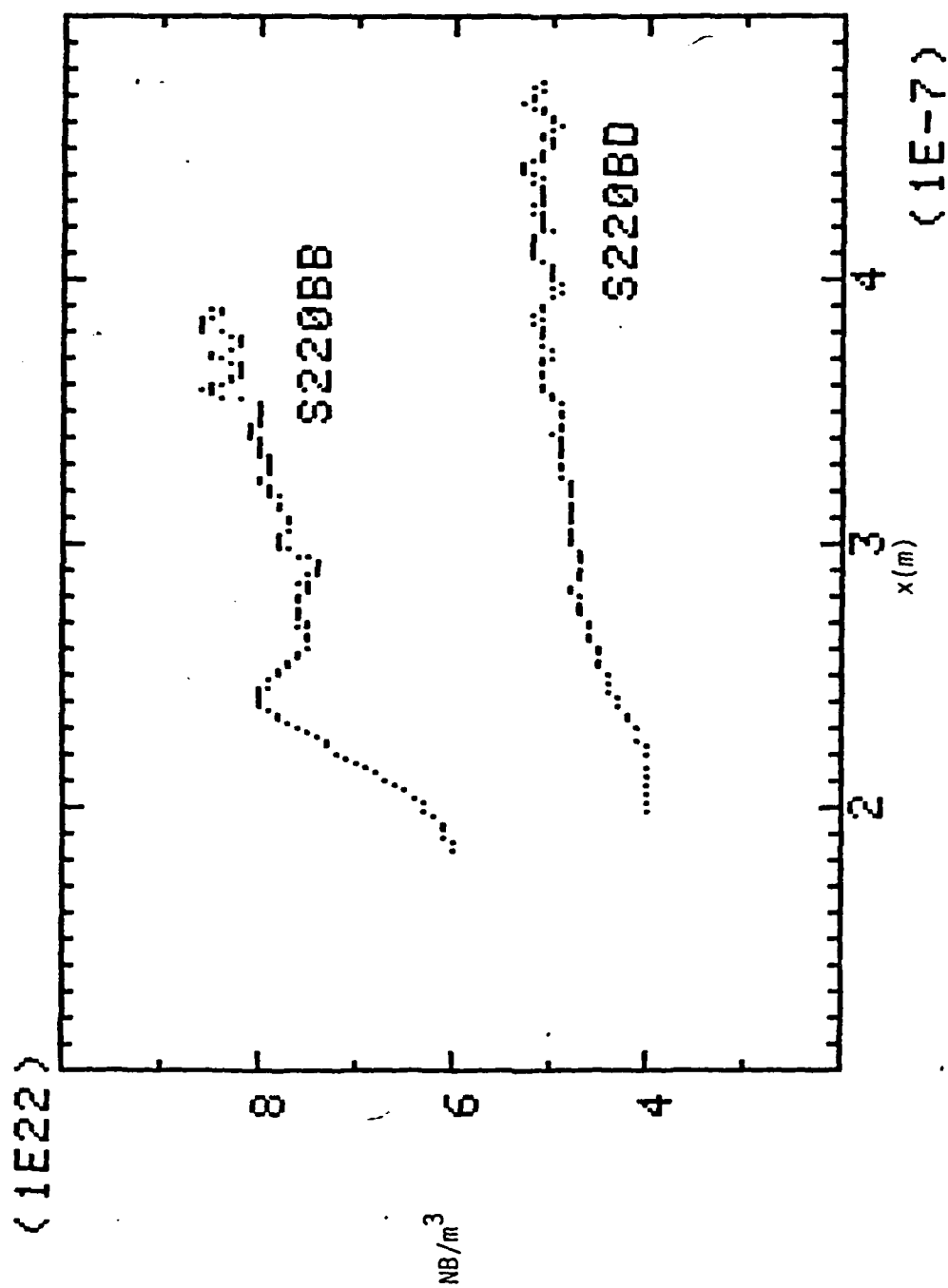


FIGURE 3: This plot shows N_B for each sample at 400K.

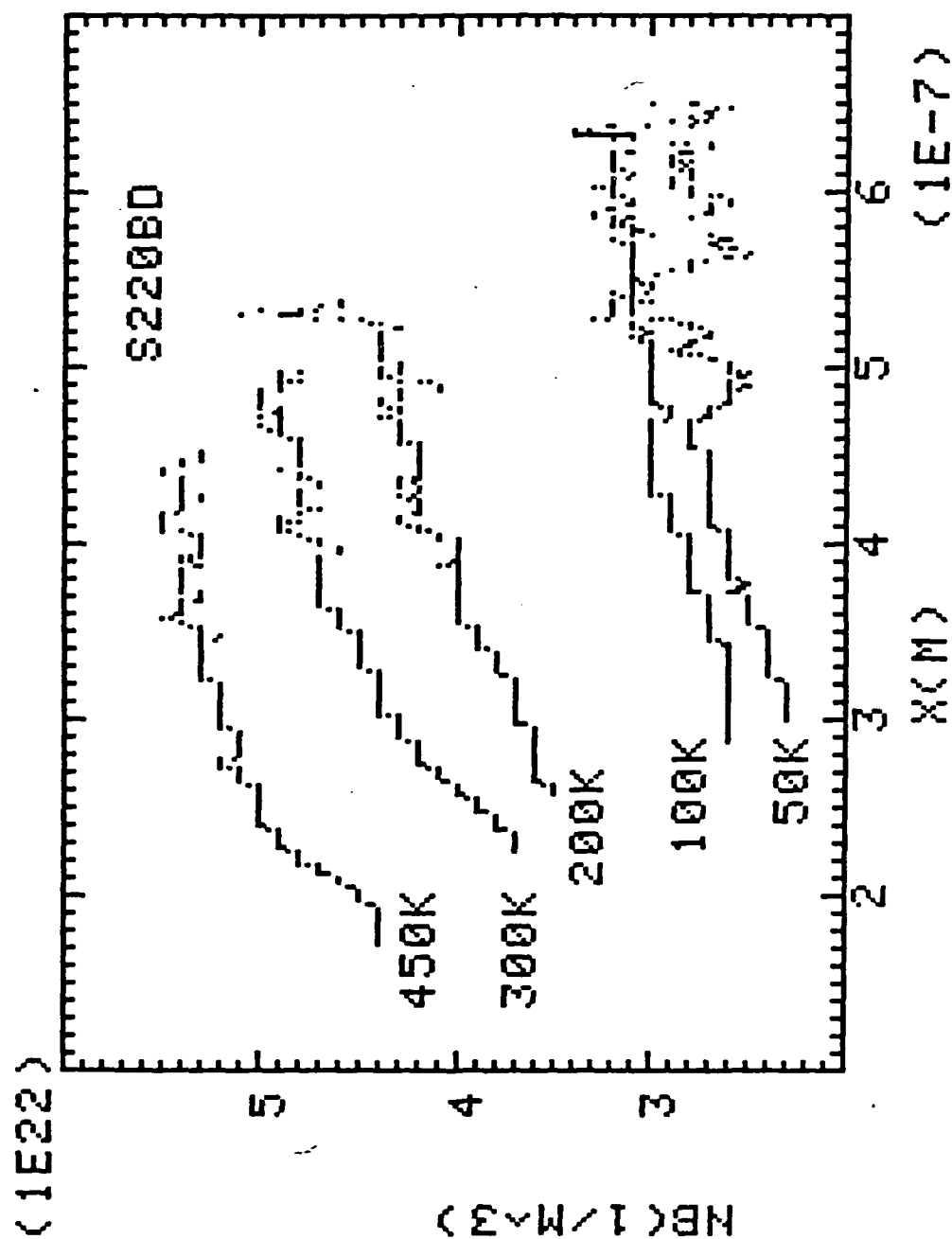


FIGURE 4: Background doping concentration, NB as a function of position in the junction for sample S220BD.

of DLTS spectrum each sample generated in order that a general feeling could be attained about what trapping states were present in each sample. Figures 5 and 6 show the general spectrum generated by each sample. As one can see, only one trapping state is shown for the non-irradiated sample. This low temperature peak ($\sim 150\text{K}$) is the DX center. The irradiated sample however shows at least six states, and they are labeled E1-E6 on Figure 6. Trap E2 is the DX center. Since both samples contained this state, it was decided to first characterize the DX center in each sample and compare the results to see if this defect was affected by irradiation. The results of subsequent DLTS runs for this peak gave an activation energy, $E_t = 0.32 \pm 0.01 \text{ eV}$ and a prefactor, $A = 3.9 \times 10^8$ (range 1.4×10^8 to 1.1×10^9), for the non-irradiated sample. For the irradiated sample, $E_t = 0.31 \pm 0.01 \text{ eV}$ and $A = 1.2 \times 10^8$ (range 4.3×10^7 to 3.2×10^8). As one can see the energies agree quite well. Also, if one considers the fact that a small change in slope on the Arrhenius plot has a large effect on the intercept, the difference in the prefactor values becomes acceptable. Any A values of the same order of magnitude can be considered to be equal for this kind of study. The similarity of these trap parameters led to the assumption that the DX center was unaffected by electron irradiation, however one more parameter was checked to verify this assumption. From equation 19, the DX center trap concentration values were calculated. S220BB had an $N_T = 4.8 \times 10^{15}/\text{cm}^3$ and S220BD had an $N_T = 2.3 \times 10^{15}/\text{cm}^3$. At first look, these values would seem to invalidate the hypothesis that the DX center was not affected, however it has been shown [7] that the amount of DX centers is so greatly affected by the aluminum mole fraction, that the value of N_T can change by more than an order of magnitude even across a single sample if the aluminum mole fraction is not constant. It is quite reasonable to assume that the aluminum mole fraction is not uniform throughout these samples, and that values of N_T that are within a factor of 3 are reasonably equal. Therefore, it was concluded that the DX center was unaffected by the electron irradiation.

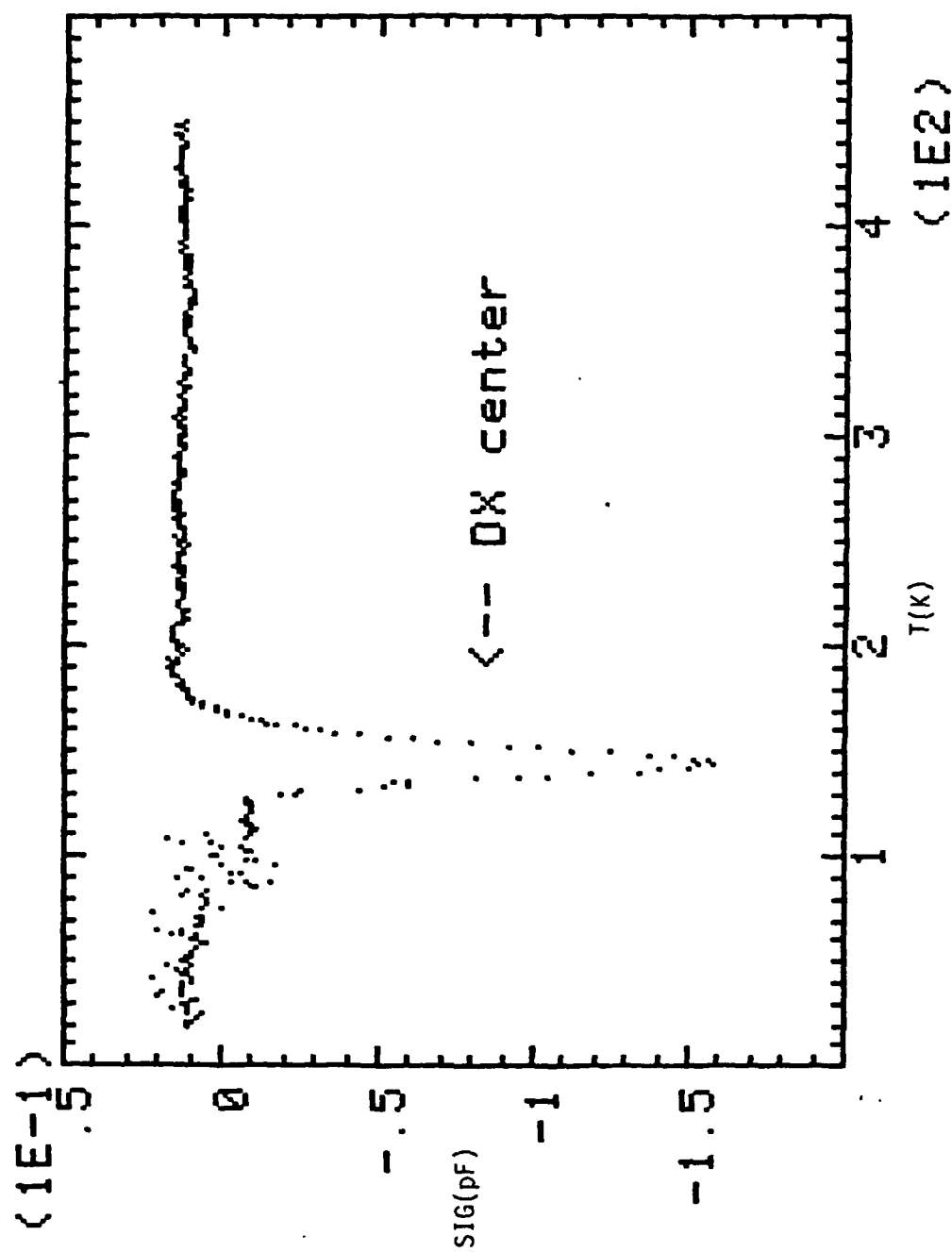


FIGURE 5: DLTS Spectrum for S220BB, pulse width of 10 ms

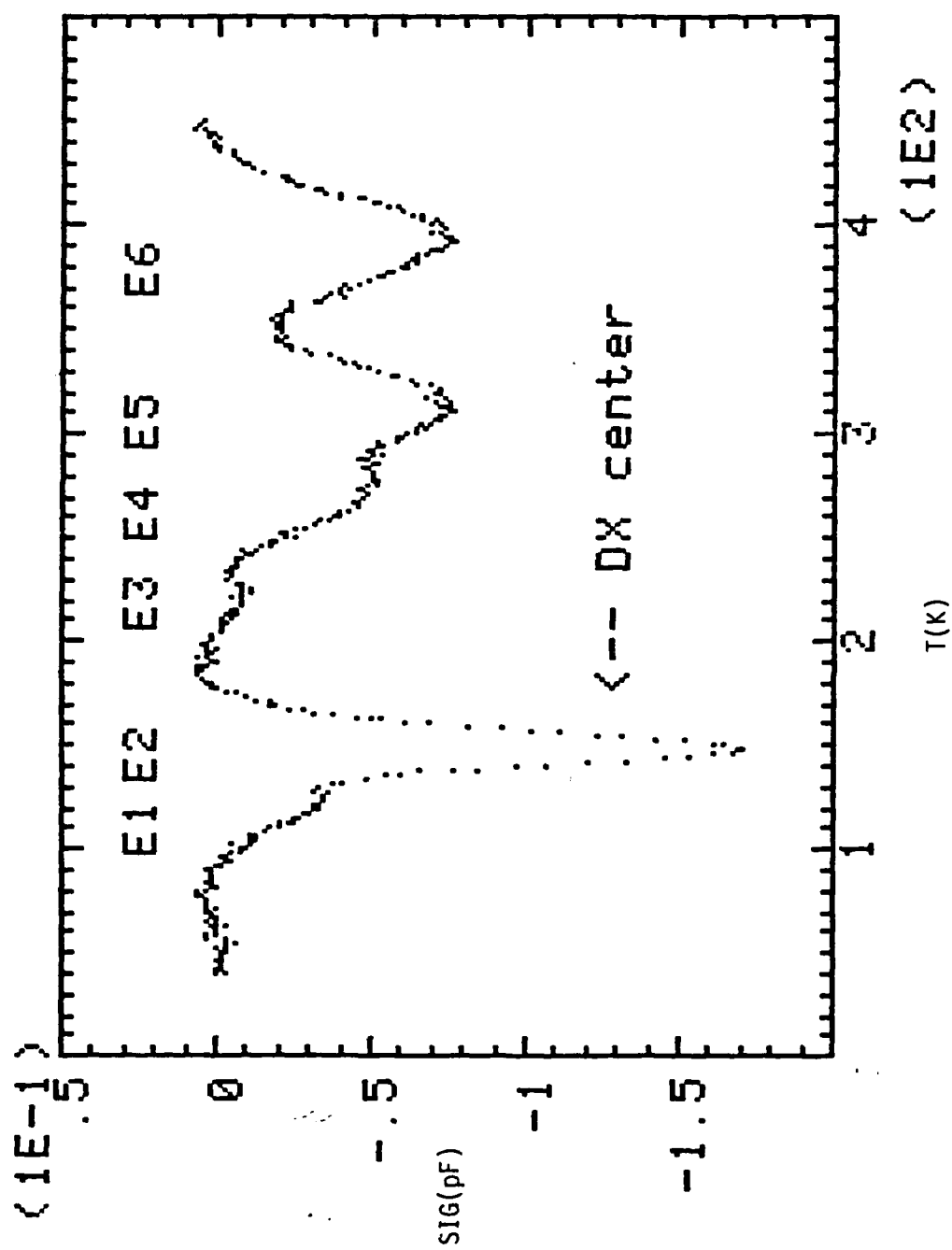


FIGURE 6: DLTS Spectrum of S2208D, pulse width of 10 ms.

After analyzing the DX center, the next task was to characterize the states seen in S220BD that were not seen in S220BB. As labeled in Figure 6, these new states are E1, and E3-E6. Since peaks E1 and E4 lay on the shoulders of E2 and E5 respectively, the first step was to try and separate the peaks so that overlap did not cause error in the ensuing analysis. By narrowing the width of the filling pulse, traps with slow capture rates would not be filled and their contribution to the DLTS signal would disappear. Using a narrow pulse width resulted in the disappearance of E2, E3 and E4 from the DLTS output. See Figure 7. Using these data, E_t and A values for traps E1, E5 and E6 were calculated. To obtain data from which to calculate these parameters for traps E3 and E4, the narrow pulse width data files were subtracted point for point from the wide pulse width files. This subtraction yielded a signal output with peaks E3 and E4 alone. E_t and A values were then obtained for these two states.

Now that the DLTS parameters had been calculated for all six states, it was time to test their validity. This was done using a computer program that would give a theoretical DLTS system output based on the input of E_t and A for each trap. Inputting the data obtained from the previous analysis yielded the output shown in Figure 8 in which it is compared to an actual DLTS run. The fit of theory to the data was not unreasonable, but there was room for improvement. The fit falls short of expectation in the regions of E1, E2 (the DX center), and E4. It has been shown [8] that the DX center is a complex defect and does not have an exponential emission rate. This means that a point defect model (single E_t , single A) based on exponential emission (which the DLTS system is) will not accurately describe the DX center. The purpose of calculating point defect parameters for E2 was merely to provide a basis for the comparisons made between the two samples. However, an attempt was made to improve the analysis in the regions of E1 and E4. A closer look at the comparison in the region of E4 (see Figure 9) suggests that there is another state between E4 and E5. This state was labeled E4A. By using point by point subtraction of the theory

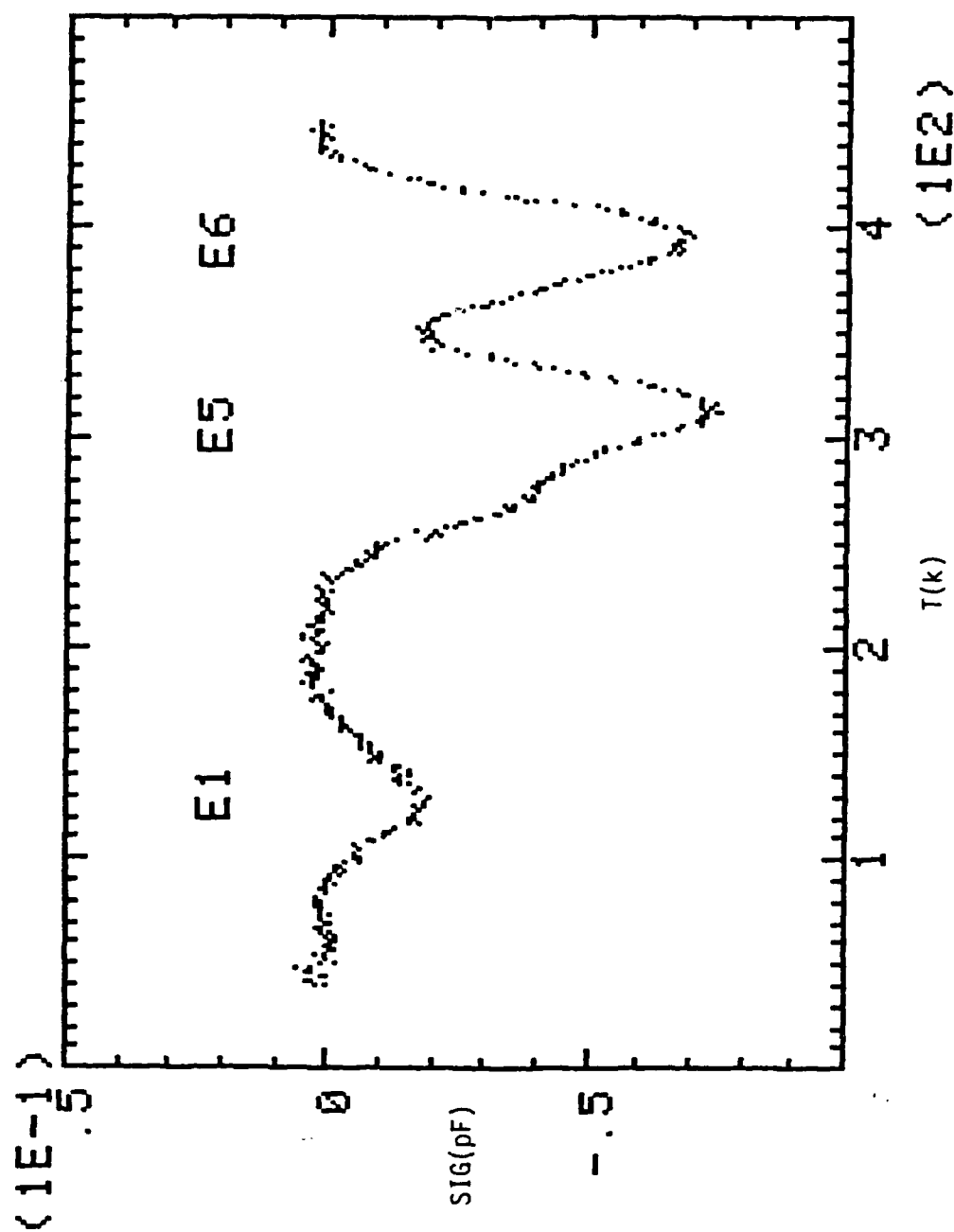


FIGURE 7: DLTS spectrum for S220BD, pulse width of 2 micro-seconds.

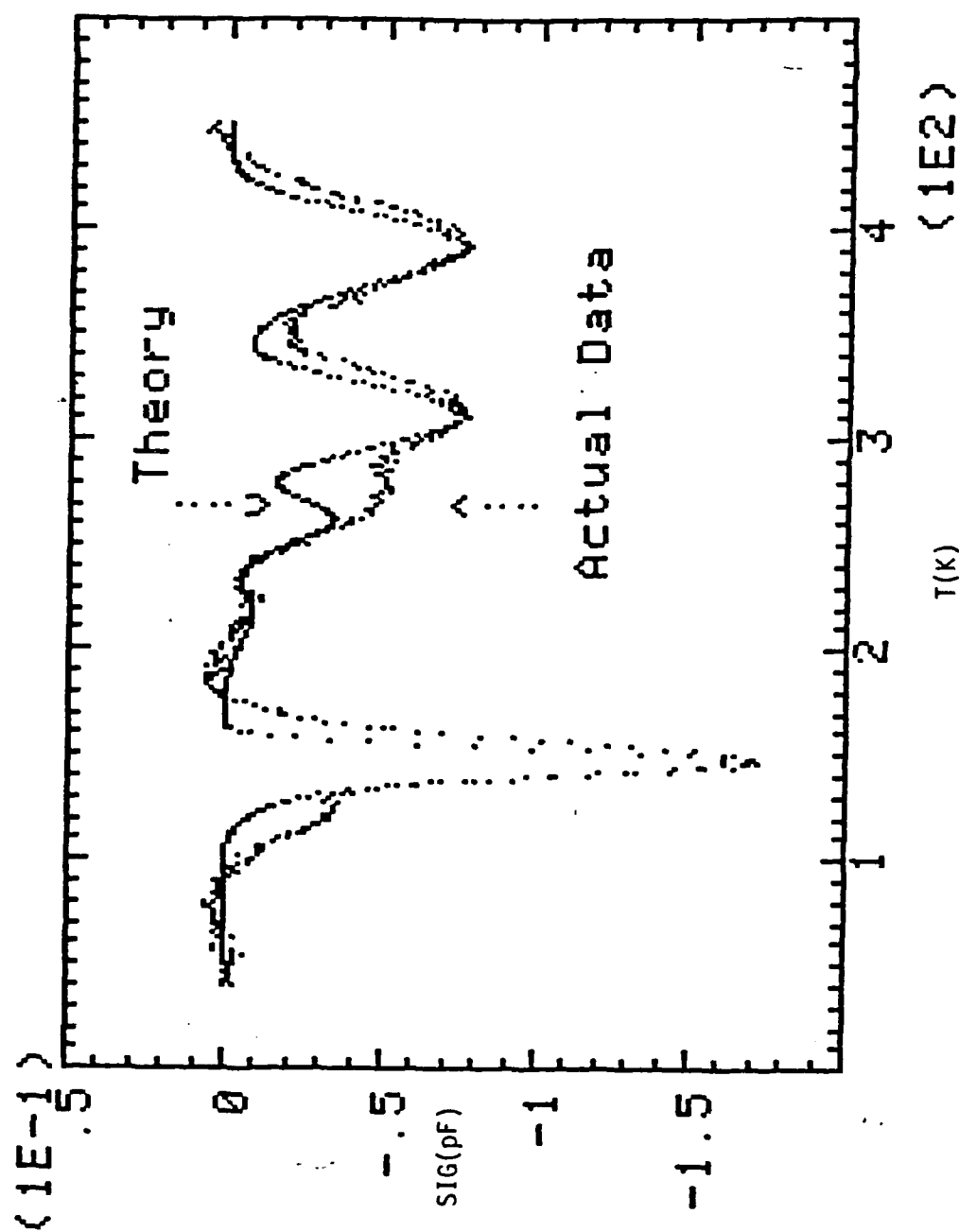


FIGURE 8: Comparison of theory to data for traps E1-E6.

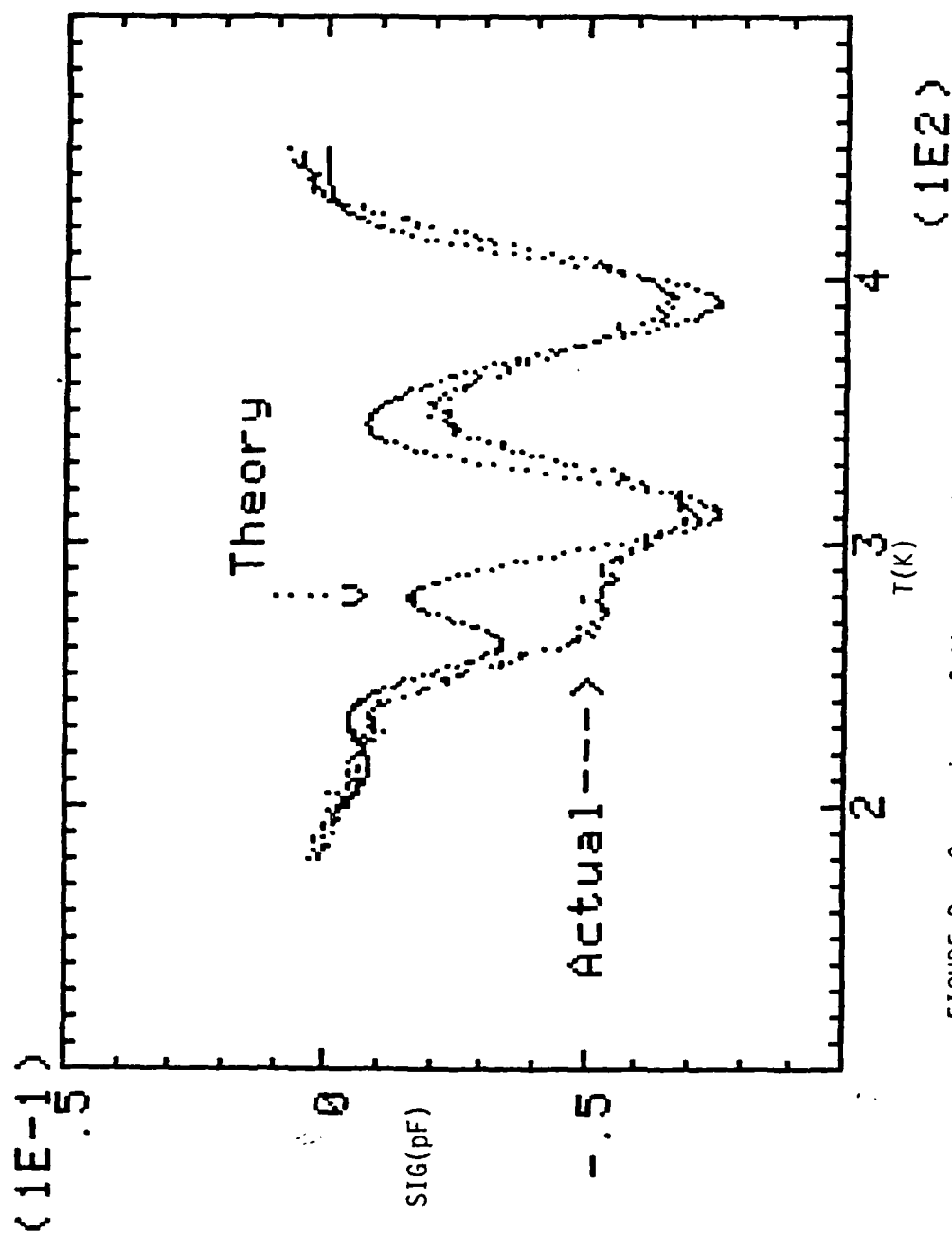


FIGURE 9: Comparison of theory to data in high temperature region, traps E3-E6.

and actual data run files, a peak for E4A was generated and analyzed. Noticing that the actual peak E1 was too broad to be a single state (see Figure 10) the same technique was used to obtain peak E1A and calculate its parameters. This revised information was used to make another theoretical DLTS output for comparison with the actual output. See Figure 11. Note that the theory matches the actual quite well, with the exception of the region around E1 and E1A. This study is willing to claim confidence for the values obtained for E4A and E3-E6, but will admit that its interpretation of the data for E1 and E1A is not unique and that there may be more physics involved in that region than can be described by the point defect modeling used in this study. A summary of parameters for all the traps analyzed is given below.

TRAP	E_t eV	A	$ N_T \times 10^{14} / \text{cm}^3 $	r 1/cm	$\sigma_{\infty} \times 10^{-16} \text{cm}^2$
E1	0.18	3.6×10^4	1.0	.01	2.4
E1A	0.15	1.6×10^4	2.2	.02	1.1
E2	0.31	1.2×10^8	19.0	N. A.	7900
E3	0.37	6.0×10^5	1.0	.01	40
E4	0.62	7.7×10^8	4.9	.05	51000
E4A	0.59	3.4×10^7	5.0	.05	2300
E5	0.60	3.0×10^6	11.5	.11	200
E6	0.85	3.4×10^7	14.5	.15	2300

TABLE 2 : Summary of DLTS trap parameters for S220BD. Trap (activation) energy, E_t ; prefactor, A; trap concentration, N_T ; introduction rate, $r = N_T / \text{fluence}$; σ_{∞} is the capture cross section at T infinity.

IV. CONCLUSIONS

The above analysis leads to the following conclusions. First, the DX center is unaffected by electron irradiation, as one might already expect given that it is a complex defect. Second, that since irradiation was effectively the only variable in the fabrication of these samples, the states seen in S220BD that were not present in S220BB were irradiation induced. Third, that since traps E3-E6, including E4A were modeled very effectively using a point defect model, they must be point defects and not complex centers.

The best hypothesis as to the nature of the defects would be due to displacements in the As sublattice resulting in As vacancies or interstitials [9]. However, comparison with data

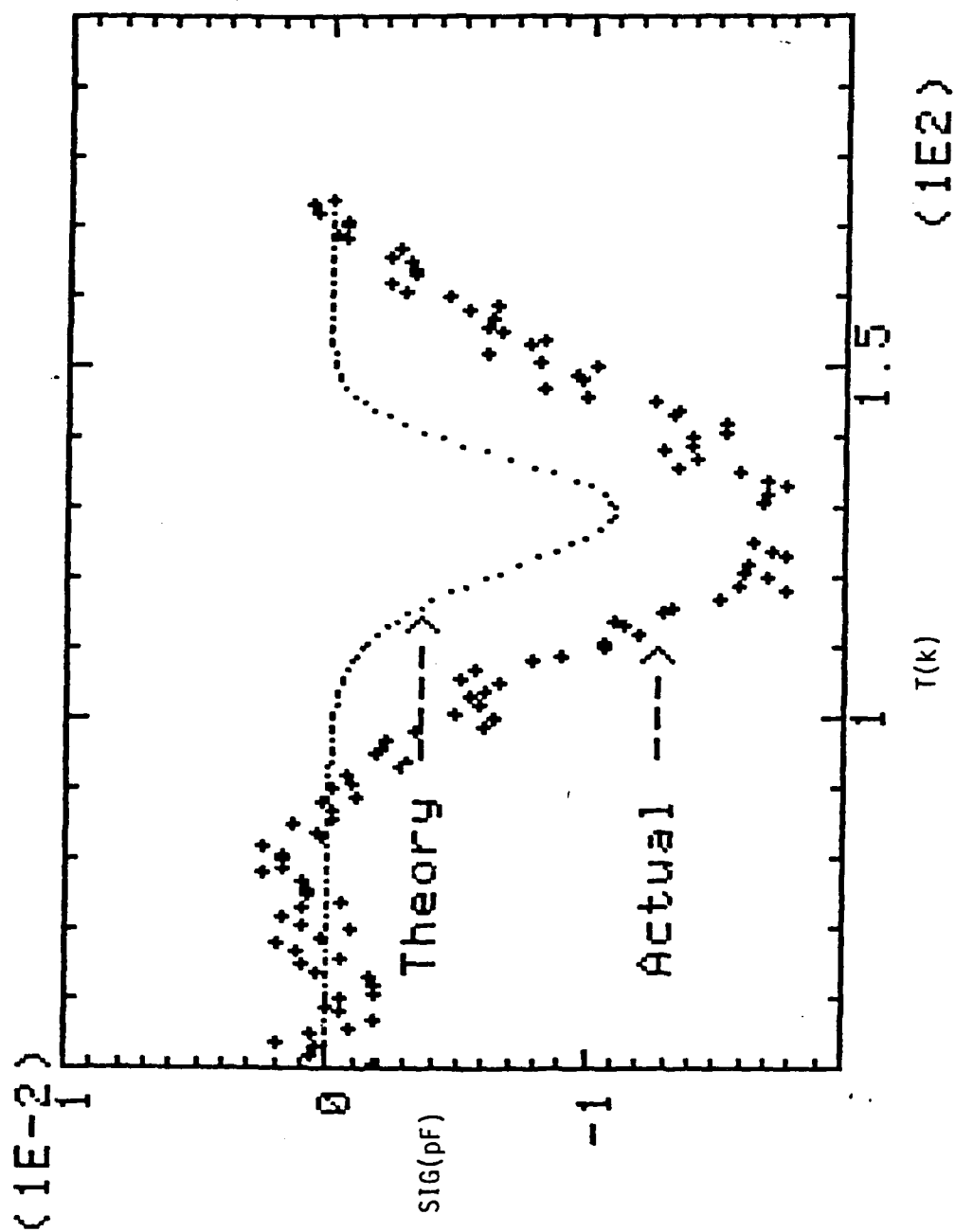


FIGURE 10: Comparison of theory to data for trap E1.

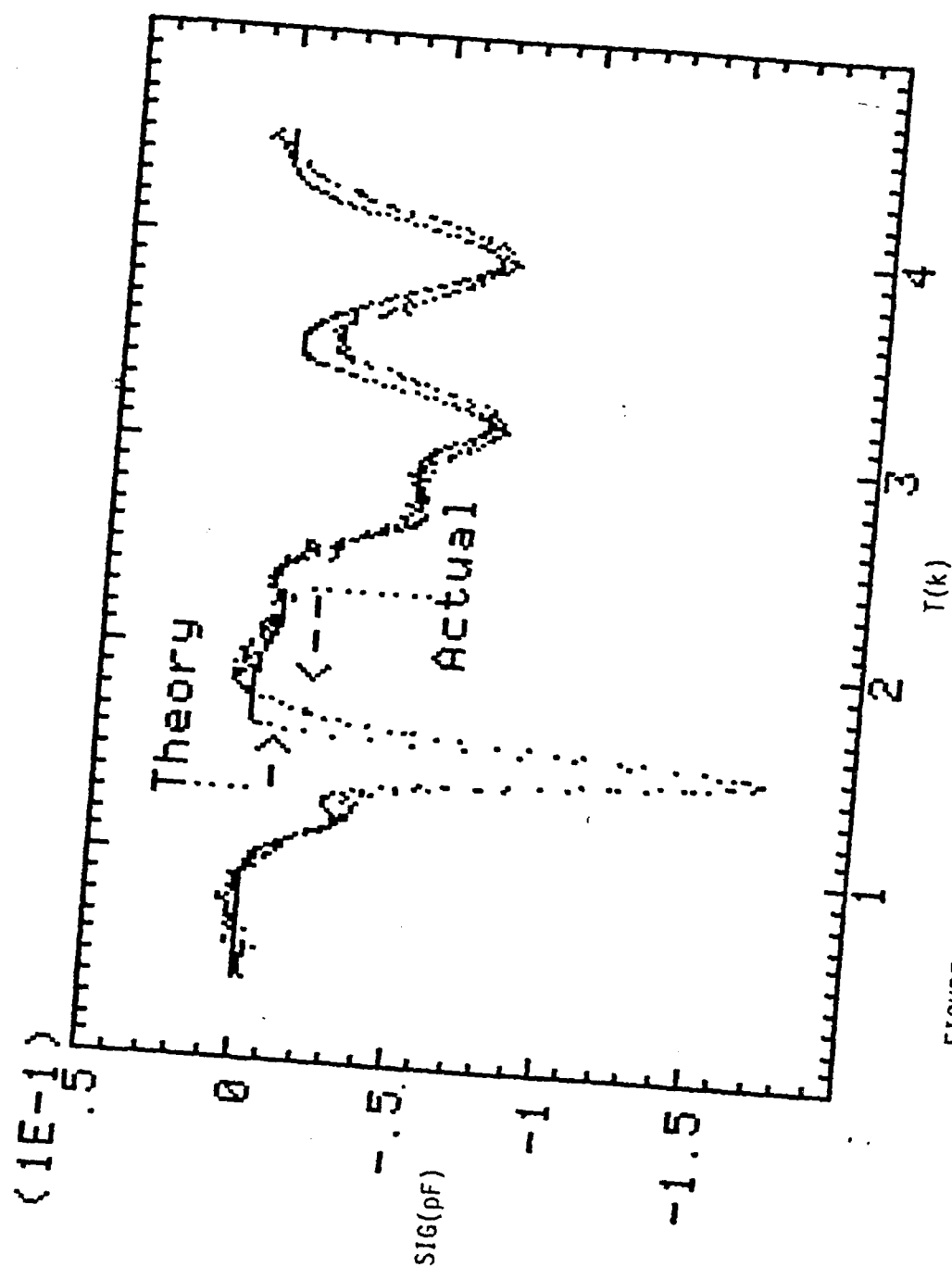


FIGURE 11: Comparison of theory to data for traps E1-E6, E1A, and E4A.

on $\text{Al}_x\text{Ga}_{1-x}\text{As}$ samples from previous work [10] on samples with other n-type dopants does not show good agreement with respect to energies, introduction rates or capture cross-sections. The best agreement with states measured by previous work is with studies by Mooney [11], where trapping states in n-type Si-doped $\text{Al}_x\text{Ga}_{1-x}\text{As}$ were measured as a function of substrate growth temperature for Molecular Beam Epitaxy (MBE) growth. This work found that lowered substrate temperature resulted in states with energies of 0.77eV, 0.62eV, 0.36eV, 0.30eV, 0.26eV and 0.18eV which are in fairly close agreement with states found in the work reported here. This comparison is not surprising since low substrate temperature can result in atoms not reaching their equilibrium positions in the growing crystal, thus resulting in native defects such as the vacancies and interstitials resulting from electron radiation.

REFERENCES

1. D. V. Lang: Phys. Rev. B19, 1015-1030 (1979)
2. D. Pons, J. C. Bourgoin: J. Phys. C: Solid State Phys. 18, 3839-3871 (1985)
3. D. V. Lang: J. App. Phys. 45, 3014-3022 (1974)
4. S. M. Sze: *Physics of Semiconductor Devices* (Wiley, New York 1969)
5. M. Lanoo, J. C. Bourgoin: *Point Defects in Semiconductors : Theoretical Aspects* (Springer, Berlin 1981)
6. H. S. Hopkins: USNA-Trident Scholar Report; no. 111, 1-58 (1981)
7. D. V. Lang: Phys. Rev. B19, 1015-1030 (1979)
8. Ibid.
9. S. Loualiche, G. Guillot, A. Nouailhat, J. C. Bourgoin: Phys. Rev. B26, 7090-7092 (1982)
10. D. V. Lang: Inst. Phys. Conf. Ser. No. 31, 70-94 (1977)
11. P. Mooney, R. Fischer, H. Morkoc: J. Appl. Phys. 57, 1928-1931 (1985)